frontiers in Earth Science

ORIGINAL RESEARCH
published: 10 September 2020
doi: 10.3389/feart.2020.00343

Leaf Waxes and Hemicelluloses in Topsoils Reflect the δ^2H and $\delta^{18}O$ Isotopic Composition of Precipitation in Mongolia

Julian Struck[1], Marcel Bliedtner[1], Paul Strobel[1], Lucas Bittner[2,3], Enkhtuya Bazarradnaa[4], Darima Andreeva[5], Wolfgang Zech[6], Bruno Glaser[3], Michael Zech[2] and Roland Zech[1]*

[1] Institute of Geography, Friedrich Schiller University Jena, Jena, Germany, [2] Heisenberg Chair of Physical Geography with Focus on Paleoenvironmental Research, Institute of Geography, Technical University of Dresden, Dresden, Germany, [3] Institute of Agronomy and Nutritional Sciences, Soil Biogeochemistry, Martin Luther University Halle-Wittenberg, Halle (Saale), Germany, [4] Institute of Plant and Agricultural Sciences, Mongolian University of Life Sciences, Ulaanbaatar, Mongolia, [5] Institute of General and Experimental Biology, Russian Acadamy of Science (RAS), Ulan-Ude, Russia, [6] Institute of Soil Science and Soil Geography, University of Bayreuth, Bayreuth, Germany

OPEN ACCESS

Edited by:
Moritz Felix Lehmann, University of Basel, Switzerland

Reviewed by:
Marco Lehmann, Paul Scherrer Institut (PSI), Switzerland
Marc-Andre Cormier, University of Oxford, United Kingdom

***Correspondence:**
Julian Struck
julian.struck@uni-jena.de

Specialty section:
This article was submitted to Biogeoscience, a section of the journal Frontiers in Earth Science

Received: *27 February 2020*
Accepted: *22 July 2020*
Published: *10 September 2020*

Citation:
Struck J, Bliedtner M, Strobel P, Bittner L, Bazarradnaa E, Andreeva D, Zech W, Glaser B, Zech M and Zech R (2020) Leaf Waxes and Hemicelluloses in Topsoils Reflect the δ^2H and $\delta^{18}O$ Isotopic Composition of Precipitation in Mongolia. Front. Earth Sci. 8:343. doi: 10.3389/feart.2020.00343

Compound-specific hydrogen and oxygen isotope analyzes on leaf wax-derived *n*-alkanes ($\delta^2H_{n\text{-alkane}}$) and the hemicellulose-derived sugar arabinose ($\delta^{18}O_{ara}$) are valuable, innovative tools for paleohydrological reconstructions. Previous calibration studies have revealed that $\delta^2H_{n\text{-alkane}}$ and $\delta^{18}O_{ara}$ reflect the isotopic composition of precipitation, but – depending on the region – may be strongly modulated by evapotranspirative enrichment. Since no calibration studies exist for semi-arid and arid Mongolia so far, we have analyzed $\delta^2H_{n\text{-alkane}}$ and $\delta^{18}O_{ara}$ in topsoils collected along a transect through Mongolia, and we compared these values with the isotopic composition of precipitation ($\delta^2H_{p\text{-WM}}$ and $\delta^{18}O_{p\text{-WM}}$, modeled data) and various climate parameters. $\delta^2H_{n\text{-alkane}}$ and $\delta^{18}O_{ara}$ are more positive in the arid south-eastern part of our transect, which reflects the fact that also the precipitation is more enriched in ^2H and ^{18}O along this part of the transect. The apparent fractionation ε_{app}, i.e., the isotopic difference between precipitation and the investigated compounds, shows no strong correlation with climate along the transect ($\varepsilon_{2H\ n\text{-}C29/p} = -129 \pm 14‰$, $\varepsilon_{2H\ n\text{-}C31/p} = -146 \pm 14‰$, and $\varepsilon_{18O\ ara/p} = +44 \pm 2‰$). Our results suggest that $\delta^2H_{n\text{-alkane}}$ and $\delta^{18}O_{ara}$ in topsoils from Mongolia reflect the isotopic composition of precipitation and are not strongly modulated by climate. Correlation with the isotopic composition of precipitation has root-mean-square errors of 13.4‰ for $\delta^2H_{n\text{-}C29}$, 12.6 for $\delta^2H_{n\text{-}C31}$, and 2.2‰ for $\delta^{18}O_{ara}$, so our findings corroborate the great potential of compound-specific $\delta^2H_{n\text{-alkane}}$ and $\delta^{18}O_{ara}$ analyzes for paleohydrological research in Mongolia.

Keywords: biomarkers, *n*-alkanes, sugars, compound-specific isotopes, apparent fractionation

INTRODUCTION

Leaf wax-derived *n*-alkanes and hemicellulose-derived sugars are produced by higher terrestrial plants and stay well-preserved in soils and sediments, because of their resistance against biochemical degradation (Eglinton and Hamilton, 1967). These compounds and their compound-specific stable hydrogen ($\delta^2H_{n\text{-alkane}}$) and oxygen ($\delta^{18}O_{sugar}$) isotopic composition get incorporated into soils through above-ground and root litter, abrasion, as well as grazing (dung), and they have a mean residence time of ∼40 years (leaf wax *n*-alkanes), while pentoses (including the hemicellulose-derived sugar arabinose) average over ∼20 years (Schmidt et al., 2011). Since $\delta^2H_{n\text{-alkane}}$ and $\delta^{18}O_{sugar}$ are not strongly affected by degradation effects (Zech et al., 2011, 2012), they are increasingly used for paleohydrological reconstructions (Aichner et al., 2015; Hepp et al., 2015, 2019; Thomas et al., 2016; Rach et al., 2017; Schäfer et al., 2018; Bliedtner et al., 2020). Usually, they are interpreted to record the isotopic composition of precipitation (Sachse et al., 2006, 2012; Tuthorn et al., 2015; Hou et al., 2018; Hepp et al., 2020), which in turn is long acknowledged as a valuable proxy for paleoclimate reconstructions and controlled by e.g., the temperature and amount effect, continentality, and altitude (Dansgaard, 1964). The isotopic signal of precipitation can be altered by isotopic fractionation at the soil-plant-atmosphere interface, including evaporative enrichment of soil water (ε_{SW}), transpirative enrichment of leaf water (ε_{Et}) and biosynthetic fractionation (ε_{bio}) (Schimmelmann et al., 2006; Sachse et al., 2012; Liu et al., 2016; Cormier et al., 2018; Liu and An, 2019).

ε_{SW} and ε_{Et} can lead to more positive $\delta^2H_{n\text{-alkane}}$ and $\delta^{18}O_{sugar}$ values relative to precipitation and/or the plants source water. ε_{SW} is probably of minor importance under semi-arid and arid conditions because most plants (especially perennial plants) exploit deeper water sources that are not isotopically affected by evaporation (Feakins and Sessions, 2010; Kahmen et al., 2013a; Berke et al., 2015), while ε_{Et} has a significant influence on $\delta^2H_{n\text{-alkane}}$ and $\delta^{18}O_{sugar}$ (Hou et al., 2008; Feakins and Sessions, 2010; Tuthorn et al., 2014, 2015; Berke et al., 2015; Cernusak et al., 2016; Liu et al., 2017). During biosynthesis, ε_{bio} leads to ^2H depletion of ∼−160‰ in $\delta^2H_{n\text{-alkane}}$ values and ^{18}O enrichment of ∼+27‰ in $\delta^{18}O_{sugar}$ values. At the same time, it is reported that ε_{bio} can vary among plant life forms and plant physiological metabolisms, for different environmental conditions and latitudes, as well as through relative contributions of the strongly depleted NADPH pool (Sessions et al., 1999; Kahmen et al., 2013b; Newberry et al., 2015; Liu et al., 2016; Sessions, 2016; Lehmann et al., 2017; Cormier et al., 2018; Griepentrog et al., 2019; Liu and An, 2019). The apparent fractionation ($\varepsilon_{2H\ n\text{-}alkane/p}$, $\varepsilon_{18O\ sugar/p}$), i.e., the difference between the isotopic signature of precipitation/source water (δ^2H_p and $\delta^{18}O_p$) and $\delta^2H_{n\text{-alkane}}$ and $\delta^{18}O_{sugar}$, respectively, basically integrates over ε_{SW}, ε_{Et} and ε_{bio} and results in ^2H-depleted leaf wax-derived *n*-alkanes but ^{18}O-enriched hemicellulose-derived sugars relative to δ^2H_p and $\delta^{18}O_p$ (Sachse et al., 2012; Tuthorn et al., 2015; Daniels et al., 2017; Liu and An, 2019; Strobel et al., 2020).

While some studies suggest that $\varepsilon_{2H\ n\text{-}alkane/p}$ in plants and topsoils remains relatively constant over latitudinal distances (Liu et al., 2016, Liu and An, 2019; Vogts et al., 2016), many others show correlations of $\varepsilon_{2H\ n\text{-}alkane/p}$ with relative humidity, mean annual precipitation (MAP) and the aridity index (AI) (Hou et al., 2008, 2018; Douglas et al., 2012; Tipple and Pagani, 2013; Berke et al., 2015; Herrmann et al., 2017; Li et al., 2019). This can be related to more evapotranspirative enrichment under more arid conditions, but plant physiological adaptations might also play a role, as well as changes in vegetation, as e.g., monocotyledons have more negative $\delta^2H_{n\text{-alkane}}$ values than dicotyledons (Sachse et al., 2012; Kahmen et al., 2013b; Hepp et al., 2020). For relatively arid regions in the United States and South Africa, Hou et al. (2008), Feakins and Sessions (2010), and Strobel et al. (2020) found no correlations of $\varepsilon_{2H\ n\text{-}alkane/p}$ with climate, and they reported constant, but quite different values (-94 ± 21‰, -99 ± 8‰, and -133 ± 12‰, respectively).

So far, only very few calibration studies applied compound-specific $\delta^{18}O_{sugar}$ analyzes (Tuthorn et al., 2015; Hepp et al., 2016, 2020; Strobel et al., 2020). For semi-arid and arid regions in South America and South Africa, Tuthorn et al. (2015) and Strobel et al. (2020) suggest enhanced evapotranspirative enrichment and higher $\varepsilon_{18O\ sugar/p}$ values with increasing aridity.

By now, $\delta^2H_{n\text{-alkane}}$ and $\delta^{18}O_{sugar}$ topsoil calibration studies on modern reference material do not exist for semi-arid and arid Mongolia, so it is not clear whether $\delta^2H_{n\text{-alkane}}$ and $\delta^{18}O_{sugar}$ reflect the isotopic composition of precipitation and/or are strongly modulated by evapotranspirative enrichment and climate conditions. Therefore, the aim of this study is to evaluate the influence of different climatic factors on the isotopic composition of leaf wax-derived *n*-alkanes ($\delta^2H_{n\text{-alkane}}$) and the hemicellulose-derived sugar arabinose ($\delta^{18}O_{ara}$) in topsoils from semi-arid and arid Mongolia. More specifically, we addressed the following research questions:

(1) Do $\delta^2H_{n\text{-alkane}}$ and $\delta^{18}O_{ara}$ reflect the isotopic composition of precipitation along the investigated transect?
(2) Do $\varepsilon_{2H\ n\text{-}alkane/p}$ and $\varepsilon_{18O\ ara/p}$ indicate a variable and climate-dependent fractionation on $\delta^2H_{n\text{-alkane}}$ and $\delta^{18}O_{ara}$?

Our study will provide the necessary basis for using $\delta^2H_{n\text{-alkane}}$ and $\delta^{18}O_{ara}$ for paleohydrological and -climatological reconstructions in semi-arid and arid Mongolia and similar regions.

MATERIALS AND METHODS

Study Area and Sampling

The semi-arid and arid regions of Mongolia are influenced by three major atmospheric circulation systems (**Figure 1A**). Summer climate is mainly dominated by the Westerlies and the East Asian summer monsoon (EASM) (Wang and Feng, 2013; Rao et al., 2015). Winter climate is dominated by the Siberian high blocking the Westerlies and thus moisture supply during winter (Yamanaka et al., 2007; Liu et al., 2009). This results in short and hot summers and long, cold, and dry winters and

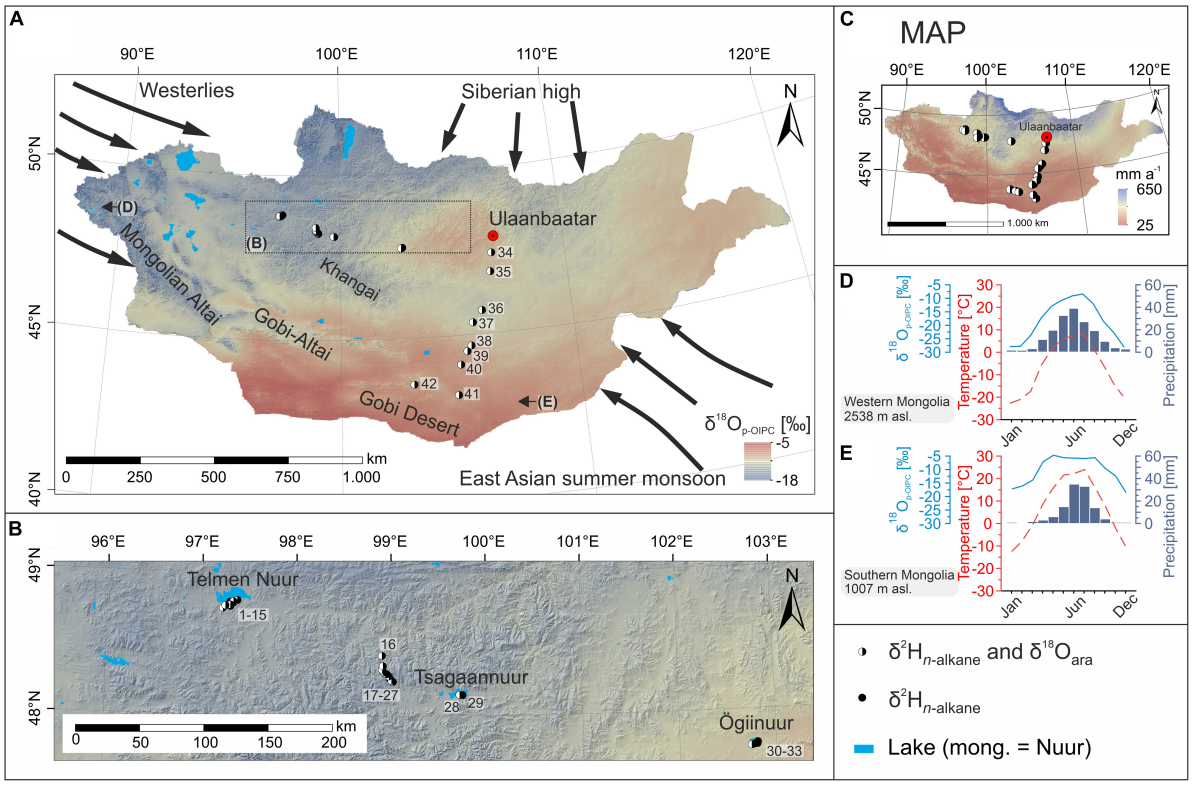

FIGURE 1 | (A) Map of Mongolia showing $\delta^{18}O_{p\text{-}OIPC}$ (Bowen, 2019) and the sampling locations. Black circles indicate samples which were analyzed for $\delta^{2}H_{n\text{-alkane}}$ only, whereas black/white circles indicate samples which were analyzed for $\delta^{2}H_{n\text{-alkane}}$ and $\delta^{18}O_{ara}$. **(B)** Submap showing a closeup of **(A)**. **(C)** Map of Mongolia showing mean annual precipitation (Fick and Hijmans, 2017). **(D,E)** Climate diagrams illustrating the seasonal variability of precipitation and temperature (1970–2000; Fick and Hijmans, 2017), as well as the variability of $\delta^{18}O_{p\text{-}OIPC}$ (Bowen, 2019) for **(D)** western Mongolia and **(E)** southern Mongolia.

overall harsh conditions (Dashkhuu et al., 2015). Especially the vegetation period, during which biosynthesis can take place, is very short and corresponds with the summer months June, July, and August, when ∼75% of the annual precipitation occurs (**Figures 1D,E**, **2H**; Lang et al., 2020).

The climate in Mongolia is characterized by increasing mean annual temperature (MAT) and decreasing mean annual precipitation (MAP) toward the south-east (**Figure 1C**). This climate gradient is mirrored in regional vegetation biomes, well-adapted to the semi-arid and arid conditions of Mongolia. Northern and central Mongolia are characterized by taiga, mountain- and forest steppe biomes, whereas steppe and desert steppe biomes are dominant in southern Mongolia (Hilbig, 1995; Klinge and Sauer, 2019). The precipitation shows a distinct $^{2}H_{p\text{-}OIPC}$ and $^{18}O_{p\text{-}OIPC}$ enrichment in southern and eastern arid Mongolia (**Figure 1A**; Bowen, 2019), and the seasonal pattern is characterized by isotopically ^{2}H- and ^{18}O-depleted precipitation during winter and ^{2}H- and ^{18}O-enriched precipitation during summer (see **Figures 1D,E** for $\delta^{18}O_{p\text{-}OIPC}$).

For this study, topsoils (0–5 cm) were sampled in LDPE plastic bags in June/July 2017 (ID: 1–33) and June 2016 (ID: 34–42). To prevent molding, samples were stored open and dark during the 2-week field campaigns. Our sampling sites were dominated by different *Poaceae* and *Cyperaceae* species (grasses) as well as herbaceous and shrubby growth forms of *Artemisia* spp. and the woody shrub *Caragana* spp. *Larix sibirica* occurred at a few sites (for more details, see Struck et al., 2020). The investigated transect follows a west-east and north-south gradient with increasing aridity and $^{2}H_{p}$ and $^{18}O_{p}$ enrichment toward eastern and southern Mongolia (**Figures 1A,B**, **2** – all sampling sites and respective climate parameters are listed in the **Supplementary Material**).

Biomarker Extraction and Chromatography

Total lipids of 42 topsoils (∼10–35 g) were extracted with dichloromethane:methanol (9:1, v/v) over three cycles using accelerated solvent extraction and ultrasonic extraction. Total lipid extracts were separated over aminopropyl pipette columns (Supelco; 45 μm), *n*-alkanes were eluted with hexane and additionally cleaned over coupled silver-nitrate ($AgNO_3$) coated silica gel (Supelco, 60–200 mesh) and zeolite (Geokleen Ltd.) pipette columns. *n*-Alkane identification and quantification were performed on an Agilent 7890B gas chromatograph equipped with an Agilent HP5MS column (30 m × 320 μm × 0.25 μm film thickness) and a flame ionization detector (GC-FID). For identification and quantification, external *n*-alkane

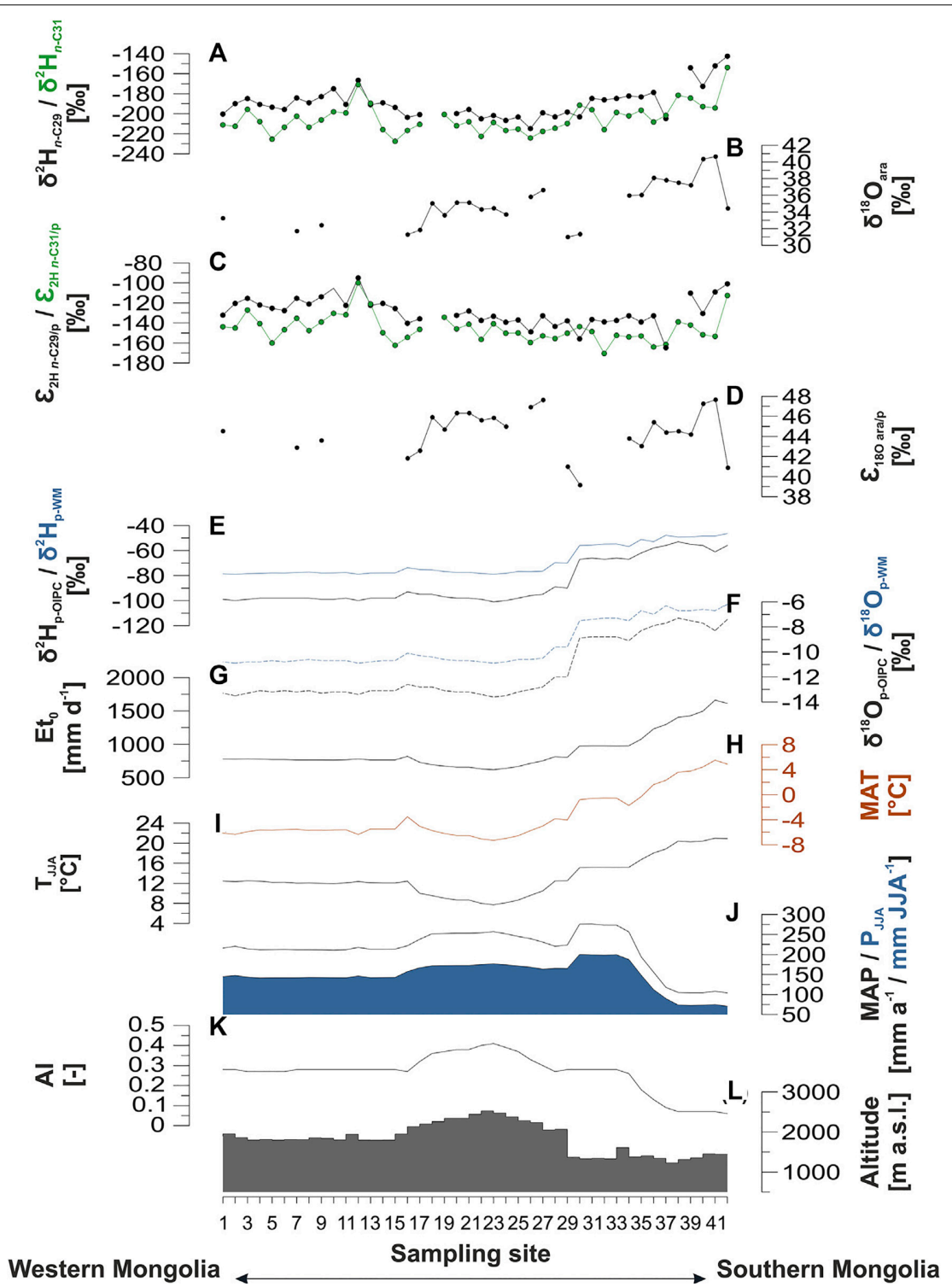

FIGURE 2 | δ^2H and $\delta^{18}O$ signatures of leaf wax-derived *n*-alkanes and the hemicellulose sugar arabinose as well as their apparent isotope fractionation (ε_{app}), compared to environmental and climatic parameters along the transect. **(A)** Compound-specific δ^2H of the leaf wax-derived *n*-alkane *n*-C_{29} (black) and *n*-C_{31} (green) (this study), **(B)** compound-specific $\delta^{18}O_{ara}$ (this study), **(C)** $\varepsilon_{2H\ n\text{-}C29/p}$ (black) and $\varepsilon_{2H\ n\text{-}C31/p}$ (green) (this study), **(D)** $\varepsilon_{18O\ ara/p}$ (this study), **(E,F)** OIPC isotopic composition of precipitation (black line) and amount-weighted isotopic signature of precipitation (blue line): δ^2H_p **(E)**, and $\delta^{18}O_p$ **(F)**, respectively (Bowen et al., 2005; IAEA/WMO, 2015; Fick and Hijmans, 2017; Bowen, 2019), **(G)** the potential evapotranspiration (Et_0) (Trabucco and Zomer, 2019), **(H)** mean annual temperature (MAP) (Fick and Hijmans, 2017), **(I)** averaged summer temperature of June, July, and August (T_{JJA}), **(J)** black line shows the mean annual precipitation (MAP), blue shaded area the summer precipitation amount (P_{JJA}) (Fick and Hijmans, 2017), **(K)** the aridity index (AI) (Trabucco and Zomer, 2019), and **(L)** the altitude (Jarvis et al., 2008).

standards (*n*-alkane mix n-C_{21} – n-C_{40}, Supelco) were measured with each sequence.

While the *n*-alkanes had been extracted and quantified in a previous study (Struck et al., 2020) and were available and ready for compound-specific δ^2H analyzes, we have selected 28 sampling sites for additional sugar analyzes. Hemicellulose-derived sugars were hydrolytically extracted from 0.1 to 1.4 g topsoil material using 10 ml of 4M trifluoroacetic acid at 105°C for 4 h according to Amelung et al. (1996). Thereafter, samples were vacuum-filtrated over glass fiber filters and the extracted sugars were cleaned over XAD-7 and Dowex 50WX8 columns to remove humic-like substances and cations (Zech and Glaser, 2009). The purified sugar samples were rotary-evaporated and derivatized with methylboronic acid (4 mg in 400 µl pyridine) at 60°C for 1 h. α-Androstane and 3-O-Methyl-Glucose were used as internal standards (Zech and Glaser, 2009).

Stable Isotope Analyzes

The compound-specific hydrogen isotopic composition of the most abundant *n*-alkanes (n-C_{29}, n-C_{31}) were measured on an Isoprime Vision isotope ratio mass spectrometer (IRMS) (Elementar, Langenselbold, Germany) coupled to an Agilent 7890B GC (Agilent, Santa Clara, United States) via a GC5 pyrolysis/combustion interface (Elementar, Langenselbold, Germany). The GC5 was operating in pyrolysis mode with a Cr (ChromeHD) reactor at 1050°C. The GC was equipped with a split/splitless injector and an Agilent HP5GC fused silica column (30 m × 320 µm × 0.25 µm film thickness). Samples were injected in splitless mode and measured as triplicates. For normalization, *n*-alkane standards (n-C_{27}, n-C_{29}, and n-C_{33}) with known isotopic composition (Schimmelmann standard, Indiana) were measured as duplicates after every third sample triplicate. All measurements were drift-corrected relative to the standards in each sequence. The H_3^+-correction factor was checked regularly throughout the sequence and yielded stable values of 3.9 ± 0.02 ($n = 4$). The standard deviation of the sample triplicates was on average 1.2 and 1.0 for n-C_{29} and for n-C_{31}, respectively, and not worse than 3.6 and 4.7‰. The standard deviation for all standards was better than 2‰ ($n = 36$). The hydrogen isotopic composition is given in delta notation (δ^2H) vs. Vienna Standard Mean Ocean Water (VSMOW).

The compound-specific oxygen isotope measurements were performed on a Trace GC 2000 coupled to a Delta V Advantage IRMS using an ^{18}O-pyrolysis reactor (GC IsoLink) and a ConFlo IV interface (all devices from Thermo Fisher Scientific, Bremen, Germany). Samples were injected in splitless mode and measured in triplicates. For normalization, derivatized sugar standards with known isotopic composition were measured repeatedly at different concentrations within every sequence. Measured $\delta^{18}O$ values were drift- and amount-corrected and corrected for the oxygen from the carbonyl group within the sugar molecules that became introduced during the hydrolysis according to Zech and Glaser (2009). The standard deviation of the sample triplicates was on average 0.4‰, and not worse than 1.2‰. The standard deviation of the arabinose standard was 1.8‰ ($n = 24$, average over four concentrations). Fucose and xylose concentrations were too low for robust isotope measurements; we therefore refrained from further evaluation of those data. The oxygen isotopic composition is given in delta notation ($\delta^{18}O$) vs. VSMOW.

DATA ANALYSIS

Apparent fractionation (ε_{app}) of hydrogen- and oxygen isotopes were calculated after Sauer et al. (2001) to test for climatic/environmental controls on $\delta^2H_{n\text{-alkane}}$ (Eq. 1) and $\delta^{18}O_{ara}$ (Eq. 2).

$$\varepsilon_{2H\ n\text{-alkane/p}} = \left(\left[\frac{\delta^2H_{n\text{-alkane}} + 1000}{\delta^2H_p + 1000}\right] - 1\right) \text{ x } 1000\ [‰] \quad (1)$$

$$\varepsilon_{18O\ ara/p} = \left(\left[\frac{\delta^{18}O_{ara} + 1000}{\delta^{18}O_p + 1000}\right] - 1\right) \text{ x } 1000\ [‰] \quad (2)$$

$\delta^2H_{p\text{-}OIPC}$ and $\delta^{18}O_{p\text{-}OIPC}$ were extracted from *The Online Isotopes in Precipitation Calculator* (OIPC, Version 3.1)[1], the uncertainty estimates (95% confidence interval) range from 1 to 8‰ for $\delta^2H_{p\text{-}OIPC}$, and from 0.2 to 0.8‰ for $\delta^{18}O_{p\text{-}OIPC}$, respectively (Bowen et al., 2005; IAEA/WMO, 2015; Bowen, 2019). Since ∼75% of the annual precipitation occurs during the vegetation period in June, July, and August, an amount-weighted mean (δ^2H_{p-WM} and $\delta^{18}O_{p-WM}$) was used to calculate $\varepsilon_{2H\ n\text{-}alkane/p}$ and $\varepsilon_{18O\ ara/p}$ (Eqs. 1, 2). MAT and MAP, as well as the temperature and precipitation of June, July and August (T_{JJA}, P_{JJA}) were extracted from the *WorldClim 2.0 dataset* (1970–2000, 30 s resolution: Fick and Hijmans, 2017)[2]. The AI and the potential evapotranspiration (Et_0) were derived from the *Global Aridity Index and Potential Evapotranspiration Climate Database v2* (1970–2000, 30 s resolution: Trabucco and Zomer, 2019)[3]. The altitude was extracted from the Shuttle Radar Topography Mission (SRTM) data (Jarvis et al., 2008).

Correlations of $\delta^2H_{n\text{-alkane}}$ and $\delta^{18}O_{ara}$ with $\delta^2H_{p\text{-}WM}$ and $\delta^{18}O_{p\text{-}WM}$, respectively were tested using weighted linear regressions. Correlations of $\varepsilon_{2H\ n\text{-}alkane/p}$ and $\varepsilon_{18O\ ara/p}$ with climate were tested using unweighted linear regressions. Goodness of fit can be assessed using R^2, and the accuracy using root-mean-square errors (RMSE). Differences between the arid part of the transect (ID: 34–42) compared to the rest were analyzed using a *t*-test. For data sets with unequal variance, the Welsh-corrected t-test was used. Statistical analyzes were done using the statistical software Origin 2019b.

RESULTS

Along our investigated transect, $\delta^2H_{n\text{-}C29}$ ranges from −215 to −143‰, with an average of -189 ± 16‰. In comparison to $\delta^2H_{n\text{-}C29}$, the $\delta^2H_{n\text{-}C31}$ values tend to be more ^2H-depleted and range from −228 to −154‰ with an average of -205 ± 15‰ (**Figure 2A**). The $\delta^{18}O_{ara}$ values range from +31‰ to +41‰ with an average of $+35 \pm 3$‰ (**Figure 2B**). All compounds

[1]http://www.waterisotopes.org

[2]http://worldclim.org/version2

[3]https://cgiarcsi.community/data/global-aridity-and-pet-database/

show the same trend as the isotopic composition of precipitation (**Figures 2E,F**), and are significantly more positive in the arid part of the transect (ID: 34 – 42) compared to the rest ($\delta^2H_{n\text{-}C29}$: $p = 0.02$, $\delta^2H_{n\text{-}C31}$: $p = 7.08e^{-4}$, $\delta^{18}O_{ara}$: $p = 2.95e^{-5}$). This reflects the ^2H and ^{18}O enrichment of the isotopic composition of precipitation, with values ranging from −101 to −53‰ for $\delta^2H_{p\text{-}OIPC}$ and from −14 to −7‰ for $\delta^{18}O_{p\text{-}OIPC}$, respectively. The amount-weighted mean values are more positive and range from −78 to −46‰ for $\delta^2H_{p\text{-}WM}$ and −11 to −6‰ for $\delta^{18}O_{p\text{-}WM}$, respectively. Like the biomarkers, the precipitation is significantly more positive in the arid part of the transect ($\delta^2H_{p\text{-}WM}$: $p = 1.39e^{-15}$, $\delta^{18}O_{p\text{-}WM}$: $p = 1.32e^{-17}$, **Figures 2E,F**).

$\varepsilon_{2H\ n\text{-}C29/p}$ ranges from −165 to −95‰ with an average of −129 ± 14‰ (**Figure 2C**). In comparison, $\varepsilon_{2H\ n\text{-}C31/p}$ is more negative, ranging from −171 to −100‰ with an average of −146 ± 14‰ (**Figure 2C**). $\varepsilon_{18O\ ara/p}$ ranges from +39‰ to +48‰ with an average of +44 ± 2‰ (**Figure 2D**). ε_{app} is not statistically different in the arid part of the transect ($\varepsilon_{2H\ n\text{-}C29/p}$: $p = 0.79$, $\varepsilon_{2H\ n\text{-}C31/p}$: $p = 0.554$, $\varepsilon_{18O\ ara/p}$: $p = 0.824$).

DISCUSSION

Differences in Compound-Specific δ^2H

Along the investigated transect $\delta^2H_{n\text{-}C29}$ is on average ∼15‰ more positive than $\delta^2H_{n\text{-}C31}$. As described previously by Struck et al. (2020), n-C_{29} is the most abundant homolog in the woody shrubs *Caragana* spp. and *Artemisia* spp., whereas n-C_{31} is the most abundant homolog in grasses. Since shrubs and dicotyledonous plants in general are more sensitive to evapotranspirative enrichment than grasses (Sachse et al., 2012; Kahmen et al., 2013b; Hepp et al., 2020), the observed offset might indicate (i) plant-physiological differences affecting the evapotranspirative enrichment of different plants, and (ii) plant-physiological differences affecting ε_{bio}.

Grasses grow via the intercalary meristem, where the leaf water is isotopically not as ^2H-enriched due to transpiration compared to the exposed part of grasses (Helliker and Ehleringer, 2000, 2002; Lehmann et al., 2017; Liu et al., 2017). The leaf wax n-alkanes, which are produced in the intercalary meristem, do therefore not incorporate the full leaf water enrichment signal (Barbour et al., 2004; Ripullone et al., 2008; Sachse et al., 2012; Kahmen et al., 2013b; Cernusak et al., 2016; Holloway-Phillips et al., 2016). This can be referred to as "dampening effect".

$\delta^2H_{n\text{-alkane}}$ and $\delta^{18}O_{ara}$ Against the Isotopic Composition of Precipitation

The $\delta^2H_{n\text{-alkane}}$ and $\delta^{18}O_{ara}$ values correlate significantly with the $\delta^2H_{p\text{-}WM}$ and $\delta^{18}O_{p\text{-}WM}$ values (**Figure 3**, $R^2 = 0.30$, $p = 3.22e^{-4}$ for $\delta^2H_{n\text{-}C29}$; 0.11 and 0.03 for $\delta^2H_{n\text{-}C31}$; and 0.36 and $1.60e^{-3}$ for $\delta^{18}O_{ara}$). Significant correlations between compound-specific biomarker isotopes and the isotopic composition of precipitation have been observed previously for different regions (a.o.: Sachse et al., 2006; Feakins and Sessions, 2010; Hou et al., 2018; Li et al., 2019; Strobel et al., 2020). In comparison to transects covering larger climate gradients (a.o. Hou et al., 2018), our determination coefficients are small and explain only up to ∼30% of the variability. However, this is due to the fact that our transect covers only a small climate gradient. The RMSE is 13.4‰ for $\delta^2H_{n\text{-}C29}$, 12.6‰ for $\delta^2H_{n\text{-}C31}$ and 2.2‰ for $\delta^{18}O_{ara}$ (**Figure 3**) and thus indicates that the biomarkers accurately record the isotopic composition of precipitation along our transect. There are several possible explanations for the observed scatter, including: (i) uncertainties related to the modeled OIPC-based isotopic composition of precipitation and the WorldClim 2.0 reanalysis

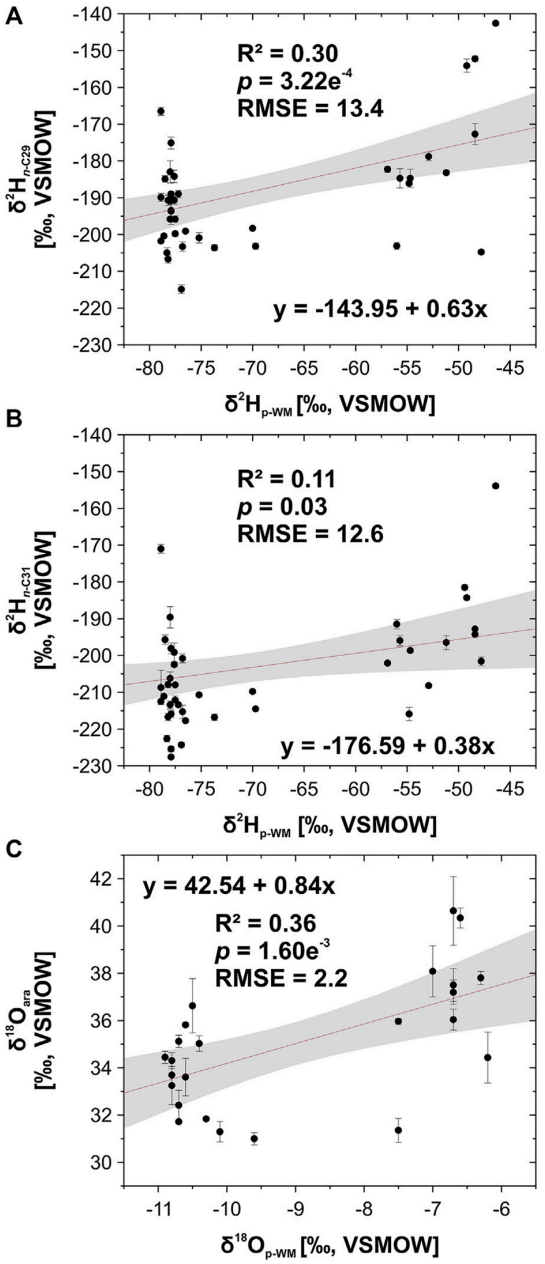

FIGURE 3 | δ^2H signatures of the leaf wax-derived n-alkanes **(A)** n-C_{29} and **(B)** n-C_{31}, as well as **(C)** $\delta^{18}O_{ara}$ signatures from the topsoil transect through Mongolia plotted against the amount-weighted δ^2H and $\delta^{18}O$ signature of precipitation ($\delta^2H_{p\text{-}WM}/\delta^{18}O_{p\text{-}WM}$). Red trend lines illustrate linear regressions, gray shaded areas the 95% confidence interval. Bold R^2/p-values indicate the level of significance ($\alpha = 0.05$).

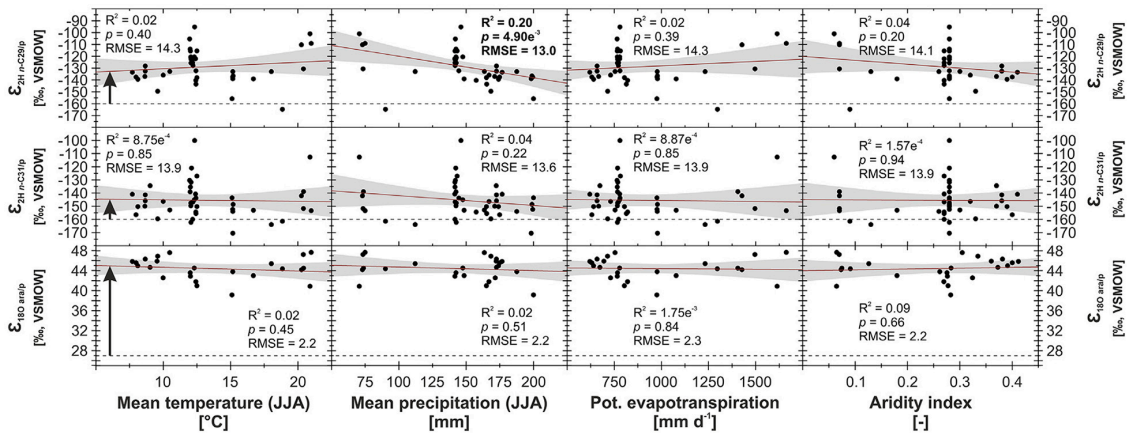

FIGURE 4 | Apparent fractionation $\varepsilon_{2H\ n\text{-}C29/p}$, $\varepsilon_{2H\ n\text{-}C31/p}$ and $\varepsilon_{18O\ ara/p}$ from the topsoil transect through Mongolia plotted against T_{JJA}, P_{JJA}, Et_0, AI (Fick and Hijmans, 2017; Trabucco and Zomer, 2019). Red trend lines illustrate linear regressions, gray shaded areas the 95% confidence interval. Bold R^2/*p*-values indicate the level of significance ($\alpha = 0.05$). Black dashed lines illustrate values for the biosynthetic fractionation, and black arrows indicate the effect of evapotranspirative enrichment (biosynthetic fractionation factors of −160 and +27‰ are assumed for the *n*-alkanes and arabinose, respectively).

dataset, (ii) the analytical errors of the $\delta^2H_{n\text{-alkane}}$ and $\delta^{18}O_{ara}$ measurements, (iii) micro-climatic effects along the investigated transect, and (iv) metabolic differences affecting ε_{bio} (Sachse et al., 2012; Fick and Hijmans, 2017; Cormier et al., 2018; Hou et al., 2018; Bowen, 2019; Strobel et al., 2020; Struck et al., 2020).

Apparent Fractionation Against Climate

To check for potential climatic influences on $\delta^2H_{n\text{-alkane}}$ and $\delta^{18}O_{ara}$, we correlated apparent fractionation against T_{JJA}, P_{JJA}, Et_0 and AI (**Figure 4**), as well as MAT, MAP, and altitude (**Supplementary Figure 1**). None of the correlations with climate is significant, except $\varepsilon_{2H\ n\text{-}C29/p}$ and precipitation, which is only weak ($R^2 = 0.20$, $p = 4.90e^{-3}$ for P_{JJA}, and $R^2 = 0.12$, $p = 0.03$ for MAP). However, if climatically-controlled one might expect that temperature, potential evapotranspiration and the degree of aridity also affect evapotranspirative enrichment and ε_{app} (Hou et al., 2018). Thus, this correlation should not be overinterpreted. We conclude that ε_{app} is nearly constant with $\varepsilon_{2H\ n\text{-}C29/p} = -129 \pm 14‰$, $\varepsilon_{2H\ n\text{-}C31/p} = -146 \pm 14‰$, and $\varepsilon_{18O\ ara/p} = +44 \pm 2‰$.

Assuming constant ε_{bio} values of −160‰ for leaf wax *n*-alkanes (Sessions et al., 1999; Hepp et al., 2020), evapotranspirative enrichment would be ∼31‰ for $\delta^2H_{n\text{-}C29}$ and ∼15‰ for $\delta^2H_{n\text{-}C31}$ (**Figure 4**). While $n\text{-}C_{29}$ is the most abundant homolog in shrubs, and $n\text{-}C_{31}$ is the most abundant homolog in grasses (Bliedtner et al., 2018; Struck et al., 2020) the observed offset in evapotranspirative enrichment most likely results from plant physiological differences described above, particularly the dampening effect. Assuming a constant ε_{bio} factor of +27‰ for arabinose (Lehmann et al., 2017; Hepp et al., 2020) evapotranspirative enrichment would be ∼17‰ for $\delta^{18}O_{ara}$. While we expect arabinose to be mainly synthesized by grasses (Mekonnen et al., 2019), we cannot quantify the contribution from other plants or roots (Schädel et al., 2010). Anyhow, for arabinose synthesized by grasses, we can expect a similar dampening effect as described above for leaf waxes, because leaf water in the leaf growth-and-differentiation zone is usually not as enriched as the exposed part of grasses (Lehmann et al., 2017; Liu et al., 2017; Hepp et al., 2020).

Comparison With Other Studies

While other calibration studies in relatively arid regions have also not found a strong climatic modulation of $\varepsilon_{2H\ n\text{-}alkane/p}$, our values ($-129 \pm 14‰$ for $\varepsilon_{2H\ n\text{-}C29/p}$ and $-146 \pm 14‰$ for $\varepsilon_{2H\ n\text{-}C31/p}$) are only comparable to those from Strobel et al. (2020), i.e., $-133 \pm 12‰$ for *n*-C31 and *n*-C33, which are much more negative than those reported by Hou et al. (2008) and Feakins and Sessions (2010), i.e., $-99 \pm 8‰$ and $-92 \pm 21‰$, respectively. Most likely, plant physiological and metabolic adaptations play an important role, as leaf waxes from C_4 plants are more enriched in ^2H than leaf waxes from C_3 plants, and dicotyledons produce more enriched leaf waxes than monocotyledons (Sachse et al., 2012; Kahmen et al., 2013b; Hepp et al., 2020). Li et al. (2019) reported very similar $\varepsilon_{2H\ n\text{-}C29/p}$ values as for Mongolia from the semi-arid and arid regions in China ($-127 \pm 10‰$ compared to $-129 \pm 14‰$), yet $\varepsilon_{2H\ n\text{-}C31/p}$ is much less negative than in Mongolia ($-133 \pm 13‰$ compared to $-146 \pm 14‰$). We suggest that this reflects the fact that C_4 grasses are more dominant in China than along our transect that is dominated by C_3 grasses (Pyankov et al., 2000). Our $\varepsilon_{2H\ n\text{-}C31/p}$ values are also very much comparable to those reported for C_3 grass sites along a transect in Europe (Hepp et al., 2020), and our $\varepsilon_{2H\ n\text{-}C29/p}$ values are in very good agreement with their $\varepsilon_{2H\ n\text{-}alkane/p}$ values for sites dominated by deciduous trees, which ones more highlights the dampening effect of C_3 grasses compared to dicotyledons.

The $\varepsilon_{18O\ ara/p}$ values for Mongolia ($44 \pm 2‰$) are very similar to values reported by Strobel et al. (2020) for relatively arid regions in South Africa. There, the more humid regions have

a significantly lower $\varepsilon_{18O\ ara/p}$ (∼37‰), quite similar to the C_3 grass sites in Europe (Hepp et al., 2020). The deciduous tree sites in Europe, however, are again characterized by more enriched $\delta^{18}O_{sugar}$ values ($\varepsilon_{18O\ sugar/p}$ = ∼43‰). All this indicates that $\delta^{18}O$ is more sensitive to evapotranspirative enrichment than δ^2H, so that climate can more strongly modulate $\delta^{18}O_{sugar}$, and again that grasses show the signal dampening much more pronounced than dicotyledons.

CONCLUSION

This study investigated compound-specific $\delta^2H_{n\text{-alkane}}$ and $\delta^{18}O_{ara}$ values in topsoils collected along a transect through semi-arid and arid Mongolia in order to evaluate to which degree they reflect variations in the isotopic signature of precipitation and/or they are affected by climate and evapotranspirative enrichment. We therefore tested for correlations of $\delta^2H_{n\text{-alkane}}$ and $\delta^{18}O_{ara}$ with $\delta^2H_{p\text{-WM}}$ and $\delta^{18}O_{p\text{-WM}}$, respectively, as well as ε_{app} with climate. We can conclude the following:

- Leaf wax-derived *n*-alkanes and the hemicellulose-derived sugar arabinose are significantly more enriched in ^2H and ^{18}O in the more arid southern and eastern parts of the transect. This reflects the changes in the isotopic composition of precipitation along the transect, and the correlations with $\delta^2H_{p\text{-WM}}$ and $\delta^{18}O_{p\text{-WM}}$ have RMSE of 13.4‰ for $\delta^2H_{n\text{-alkane}}$ and 2.2‰ for $\delta^{18}O_{ara}$.
- The apparent fractionation remains mostly constant at −129 ± 14‰, −146 ± 14‰, and at +44 ± 2‰ for $\varepsilon_{2H\ n\text{-}C29/p}$, $\varepsilon_{2H\ n\text{-}C31/p}$ and $\varepsilon_{18O\ ara/p}$, respectively. There are no significant differences along the transect, nor strong correlations with climate.

Compound-specific $\delta^2H_{n\text{-alkane}}$ and $\delta^{18}O_{ara}$ analyzes on terrestrial biomarkers, preserved e.g., in lake sediments, have great potential for reconstructing past changes in the isotopic composition of precipitation and thus for paleoclimate and -hydrological reconstructions in Mongolia.

DATA AVAILABILITY STATEMENT

The datasets presented in this study can be found in the article/**Supplementary Material**.

AUTHOR CONTRIBUTIONS

JS, MB, PS, MZ, and RZ designed the study. MB and RZ collected the samples along transect I in 2016. JS and RZ collected the samples along transect II in 2017. JS carried out the major part of the laboratory analyzes in the laboratory of RZ and BG, assisted by LB, PS, and MB. EB, DA, and WZ organized the sample logistics in 2016 and 2017. JS wrote the manuscript with contributions of all coauthors. All authors contributed to the article and approved the submitted version.

FUNDING

This research was supported by the SNF (Grant No. PP00P2 – 150590).

ACKNOWLEDGMENTS

We thank the Swiss National Science Foundation (SNF) for funding. PS acknowledges the support by a fellowship from the state of Thuringia (Landesgraduiertenstipendium). DA gratefully acknowledges the support of the framework of Goszadanie no. AAAA-A17-117011810038-7. Furthermore, we greatly acknowledge M. Benesch (Martin Luther University Halle-Wittenberg) for compound-specific $\delta^{18}O$ measurements and N. Ueberschaar (MS platform, Friedrich-Schiller-University Jena) for providing laboratory facilities. I. K. Schäfer (Agilent) and J. Wintel (Elementar) are acknowledged for support during δ^2H measurements. We want to acknowledge H. Maennicke, C. Heinrich, T. Bromm, S. Polifka, M. Lerch (all Martin Luther University Halle-Wittenberg), M. Wagner, F. Freitag, I. Paetz, and N. Blaubach (all Friedrich-Schiller-University Jena) for laboratory support. We thank our logistic partners in Mongolia, especially G. Gereltsogt from Remote Mongolian Adventures and all field trip participants 2016 and 2017. We thank ML and M-AC for their valuable and helpful comments on this manuscript.

SUPPLEMENTARY MATERIAL

The Supplementary Material for this article can be found online at: https://www.frontiersin.org/articles/10.3389/feart.2020.00343/full#supplementary-material

REFERENCES

Aichner, B., Feakins, S. J., Lee, J. E., Herzschuh, U., and Liu, X. (2015). High-resolution leaf wax carbon and hydrogen isotopic record of the late Holocene paleoclimate in arid Central Asia. *Clim. Past* 11, 619–633. doi: 10.5194/cp-11-619-2015

Amelung, W., Cheshire, M. V., and Guggenberger, G. (1996). Determination of neutral and acidic sugars in soil by capillary gas-liquid chromatography after trifluoroacetic acid hydrolysis. *Soil Biol. Biochem.* 28, 1631–1639. doi: 10.1016/S0038-0717(96)00248-9

Barbour, M. M., Roden, J. S., Farquhar, G. D., and Ehleringer, J. R. (2004). Expressing leaf water and cellulose oxygen isotope ratios as enrichment above source water reveals evidence of a Péclet effect. *Oecologia* 138, 426–435. doi: 10.1007/s00442-003-1449-3

Berke, M. A., Tipple, B. J., Hambach, B., and Ehleringer, J. R. (2015). Life form-specific gradients in compound-specific hydrogen isotope ratios of modern leaf waxes along a North American Monsoonal transect. *Oecologia* 179, 981–997. doi: 10.1007/s00442-015-3432-1

Bliedtner, M., Schäfer, I. K., Zech, R., and von Suchodoletz, H. (2018). Leaf wax *n*-alkanes in modern plants and topsoils from eastern Georgia (Caucasus) – implications for reconstructing regional paleovegetation. *Biogeosciences* 15, 3927–3936. doi: 10.5194/bg-15-3927-2018

Bliedtner, M., Zech, R., Zech, J., Schäfer, I., and Suchodoletz, H. (2020). A first Holocene leaf wax isotope-based paleoclimate record from the semi-humid

to semi-arid south-eastern Caucasian lowlands. *J. Quatern. Sci.* 35, 625–633. doi: 10.1002/jqs.3210

Bowen, G. J. (2019). *The Online Isotopes in Precipitation Calculator, version 3.1*. Available online at: http://www.waterisotopes.org (accessed January 31, 2020).

Bowen, G. J., Wassenaar, L. I., and Hobson, K. A. (2005). Global application of stable hydrogen and oxygen isotopes to wildlife forensics. *Oecologia* 143, 337–348. doi: 10.1007/s00442-004-1813-y

Cernusak, L. A., Barbour, M. M., Arndt, S. K., Cheesman, A. W., English, N. B., Feild, T. S., et al. (2016). Stable isotopes in leaf water of terrestrial plants. *Plant Cell Environ.* 39, 1087–1102. doi: 10.1111/pce.12703

Cormier, M.-A., Werner, R. A., Sauer, P. E., Gröcke, D. R., Leuenberger, M. C., Wieloch, T., et al. (2018). ^{2}H-fractionations during the biosynthesis of carbohydrates and lipids imprint a metabolic signal on the δ^{2}H values of plant organic compounds. *New Phytol.* 218, 479–491. doi: 10.1111/nph.15016

Daniels, W. C., Russell, J. M., Giblin, A. E., Welker, J. M., Klein, E. S., and Huang, Y. (2017). Hydrogen isotope fractionation in leaf waxes in the Alaskan Arctic tundra. *Geochim. Cosmochim. Acta* 213, 216–236. doi: 10.1016/j.gca.2017.06.028

Dansgaard, W. (1964). Stable isotopes in precipitation. *Tellus* 16, 436–468. doi: 10.1111/j.2153-3490.1964.tb00181.x

Dashkhuu, D., Kim, J. P., Chun, J. A., and Lee, W.-S. (2015). Long-term trends in daily temperature extremes over Mongolia. *Weather Clim. Extremes* 8, 26–33. doi: 10.1016/j.wace.2014.11.003

Douglas, P. M. J., Pagani, M., Brenner, M., Hodell, D. A., and Curtis, J. H. (2012). Aridity and vegetation composition are important determinants of leaf-wax δD values in southeastern Mexico and Central America. *Geochim. Cosmochim. Acta* 97, 24–45. doi: 10.1016/j.gca.2012.09.005

Eglinton, G., and Hamilton, R. J. (1967). Leaf epicuticular waxes. *Science* 156, 1322–1335. doi: 10.1126/science.156.3780.1322

Feakins, S. J., and Sessions, A. L. (2010). Controls on the D/H ratios of plant leaf waxes in an arid ecosystem. *Geochim. Cosmochim. Acta* 74, 2128–2141. doi: 10.1016/j.gca.2010.01.016

Fick, S. E., and Hijmans, R. J. (2017). WorldClim 2: new 1-km spatial resolution climate surfaces for global land areas. *Int. J. Climatol.* 37, 4302–4315. doi: 10.1002/joc.5086

Griepentrog, M., Wispelaere, L., de Bauters, M., Bodé, S., Hemp, A., Verschuren, D., et al. (2019). Influence of plant growth form, habitat and season on leaf-wax *n*-alkane hydrogen-isotopic signatures in equatorial East Africa. *Geochim. Cosmochim. Acta* 263, 122–139. doi: 10.1016/j.gca.2019.08.004

Helliker, B. R., and Ehleringer, J. R. (2000). Establishing a grassland signature in veins: ^{18}O in the leaf water of C_3 and C_4 grasses. *PNAS* 97, 7894–7898. doi: 10.1073/pnas.97.14.7894

Helliker, B. R., and Ehleringer, J. R. (2002). Differential ^{18}O enrichment of leaf cellulose in C_3 versus C_4 grasses. *Funct. Plant Biol.* 29:435. doi: 10.1071/PP01122

Hepp, J., Rabus, M., Anhäuser, T., Bromm, T., Laforsch, C., Sirocko, F., et al. (2016). A sugar biomarker proxy for assessing terrestrial versus aquatic sedimentary input. *Organ. Geochem.* 98, 98–104. doi: 10.1016/j.orggeochem.2016.05.012

Hepp, J., Schäfer, I. K., Lanny, V., Franke, J., Bliedtner, M., Rozanski, K., et al. (2020). Evaluation of bacterial glycerol dialkyl glycerol tetraether and ^{2}H–^{18}O biomarker proxies along a central European topsoil transect. *Biogeosciences* 17, 741–756. doi: 10.5194/bg-17-741-2020

Hepp, J., Tuthorn, M., Zech, R., Mügler, I., Schlütz, F., Zech, W., et al. (2015). Reconstructing lake evaporation history and the isotopic composition of precipitation by a coupled δ^{18}O–δ^{2}H biomarker approach. *J. Hydrol.* 529, 622–631. doi: 10.1016/j.jhydrol.2014.10.012

Hepp, J., Wüthrich, L., Bromm, T., Bliedtner, M., Schäfer, I. K., Glaser, B., et al. (2019). How dry was the younger dryas? Evidence from a coupled δ^{2}H–δ^{18}O biomarker paleohygrometer applied to the gemündener maar sediments, western eifel, Germany. *Clim. Past* 15, 713–733. doi: 10.5194/cp-15-713-2019

Herrmann, N., Boom, A., Carr, A. S., Chase, B. M., West, A. G., Zabel, M., et al. (2017). Hydrogen isotope fractionation of leaf wax *n*-alkanes in southern African soils. *Organ. Geochem.* 109, 1–13. doi: 10.1016/j.orggeochem.2017.03.008

Hilbig, W. (1995). *The Vegetation of Mongolia*. Amsterdam: SPB Acad. Publ.

Holloway-Phillips, M., Cernusak, L. A., Barbour, M., Song, X., Cheesman, A., Munksgaard, N., et al. (2016). Leaf vein fraction influences the Péclet effect and ^{18}O enrichment in leaf water. *Plant Cell Environ.* 39, 2414–2427. doi: 10.1111/pce.12792

Hou, J., D'Andrea, W. J., and Huang, Y. (2008). Can sedimentary leaf waxes record D/H ratios of continental precipitation? Field, model, and experimental assessments. *Geochim. Cosmochim. Acta* 72, 3503–3517. doi: 10.1016/j.gca.2008.04.030

Hou, J., Tian, Q., and Wang, M. (2018). Variable apparent hydrogen isotopic fractionation between sedimentary *n*-alkanes and precipitation on the Tibetan Plateau. *Organ. Geochem.* 122, 78–86. doi: 10.1016/j.orggeochem.2018.05.011

IAEA/WMO (2015). *Global Network of Isotopes in Precipitation: The GNIP Database*. Available online at: https://nucleus.iaea.org/wiser (accessed January 31, 2020).

Jarvis, A., Reuter, H. I., Nelson, A., and Guevara, E. (2008). *Hole-Filled Seamless SRTM Data V4, International Centre for Tropical Agriculture (CIAT)*. Available online at: http://srtm.csi.cgiar.org (accessed January 31, 2020).

Kahmen, A., Hoffmann, B., Schefuß, E., Arndt, S. K., Cernusak, L. A., West, J. B., et al. (2013a). Leaf water deuterium enrichment shapes leaf wax *n*-alkane δD values of angiosperm plants II: observational evidence and global implications. *Geochim. Cosmochim. Acta* 111, 50–63. doi: 10.1016/j.gca.2012.09.004

Kahmen, A., Schefuß, E., and Sachse, D. (2013b). Leaf water deuterium enrichment shapes leaf wax *n*-alkane δD values of angiosperm plants I: experimental evidence and mechanistic insights. *Geochim. Cosmochim. Acta* 111, 39–49. doi: 10.1016/j.gca.2012.09.003

Klinge, M., and Sauer, D. (2019). Spatial pattern of Late Glacial and Holocene climatic and environmental development in Western Mongolia – A critical review and synthesis. *Quatern. Sci. Rev.* 210, 26–50. doi: 10.1016/j.quascirev.2019.02.020

Lang, B., Ahlborn, J., Oyunbileg, M., Geiger, A., von Wehrden, H., Wesche, K., et al. (2020). Grazing effects on intraspecific trait variability vary with changing precipitation patterns in Mongolian rangelands. *Ecol. Evol.* 10, 678–691. doi: 10.1002/ece3.5895

Lehmann, M. M., Gamarra, B., Kahmen, A., Siegwolf, R. T. W., and Saurer, M. (2017). Oxygen isotope fractionations across individual leaf carbohydrates in grass and tree species. *Plant Cell Environ.* 40, 1658–1670. doi: 10.1111/pce.12974

Li, Y., Yang, S., Luo, P., and Xiong, S. (2019). Aridity-controlled hydrogen isotope fractionation between soil *n*-alkanes and precipitation in China. *Organ. Geochem.* 133, 53–64. doi: 10.1016/j.orggeochem.2019.04.009

Liu, H. T., Schäufele, R., Gong, X. Y., and Schnyder, H. (2017). The δ^{18}O and δ^{2}H of water in the leaf growth-and-differentiation zone of grasses is close to source water in both humid and dry atmospheres. *New Phytol.* 214, 1423–1431. doi: 10.1111/nph.14549

Liu, J., and An, Z. (2019). Variations in hydrogen isotopic fractionation in higher plants and sediments across different latitudes: implications for paleohydrological reconstruction. *Sci. Total Environ.* 650, 470–478. doi: 10.1016/j.scitotenv.2018.09.047

Liu, J., Liu, W., An, Z., and Yang, H. (2016). Different hydrogen isotope fractionations during lipid formation in higher plants: implications for paleohydrology reconstruction at a global scale. *Sci. Rep.* 6:19711. doi: 10.1038/srep19711

Liu, J., Song, X., Sun, X., Yuan, G., Liu, X., and Wang, S. (2009). Isotopic composition of precipitation over Arid Northwestern China and its implications for the water vapor origin. *J. Geograph. Sci.* 19, 164–174. doi: 10.1007/s11442-009-0164-3

Mekonnen, B., Zech, W., Glaser, B., Lemma, B., Bromm, T., Nemomissa, S., et al. (2019). Chemotaxonomic patterns of vegetation and soils along altitudinal transects of the Bale Mountains, Ethiopia, and implications for paleovegetation reconstructions – Part 1: stable isotopes and sugar biomarkers. *E&G Quatern. Sci. J.* 68, 177–188. doi: 10.5194/egqsj-68-177-2019

Newberry, S. L., Kahmen, A., Dennis, P., and Grant, A. (2015). *n*-Alkane biosynthetic hydrogen isotope fractionation is not constant throughout the growing season in the riparian tree Salix viminalis. *Geochim. Cosmochim. Acta* 165, 75–85. doi: 10.1016/j.gca.2015.05.001

Pyankov, V. I., Gunin, P. D., Tsoog, S., and Black, C. C. (2000). C_4 plants in the vegetation of Mongolia: their natural occurrence and geographical distribution in relation to climate. *Oecologia* 123, 15–31. doi: 10.1007/s004420050985

Rach, O., Engels, S., Kahmen, A., Brauer, A., Martín-Puertas, C., van Geel, B., et al. (2017). Hydrological and ecological changes in western Europe between 3200 and 2000 years BP derived from lipid biomarker δD values in lake Meerfelder Maar sediments. *Quatern. Sci. Rev.* 172, 44–54. doi: 10.1016/j.quascirev.2017.07.019

Rao, M. P., Davi, N. K., D'Arrigo, R. D., Skees, J., Nachin, B., Leland, C., et al. (2015). Dzuds, droughts, and livestock mortality in Mongolia. *Environ. Res. Lett.* 10:74012. doi: 10.1088/1748-9326/10/7/074012

Ripullone, F., Matsuo, N., Stuart-Williams, H., Wong, S. C., Borghetti, M., Tani, M., et al. (2008). Environmental effects on oxygen isotope enrichment of leaf water in cotton leaves. *Plant Physiol.* 146, 729–736. doi: 10.1104/pp.107.105643

Sachse, D., Billault, I., Bowen, G. J., Chikaraishi, Y., Dawson, T. E., Feakins, S. J., et al. (2012). Molecular paleohydrology: interpreting the hydrogen-isotopic composition of lipid biomarkers from photosynthesizing organisms. *Annu. Rev. Earth Planet. Sci.* 40, 221–249. doi: 10.1146/annurev-earth-042711-105535

Sachse, D., Radke, J., and Gleixner, G. (2006). δD values of individual *n*-alkanes from terrestrial plants along a climatic gradient – Implications for the sedimentary biomarker record. *Organ. Geochem.* 37, 469–483. doi: 10.1016/j.orggeochem.2005.12.003

Sauer, P. E., Eglinton, T. I., Hayes, J. M., Schimmelmann, A., and Sessions, A. L. (2001). Compound-specific D/H ratios of lipid biomarkers from sediments as a proxy for environmental and climatic conditions. *Geochim. Cosmochim. Acta* 65, 213–222. doi: 10.1016/S0016-7037(00)00520-2

Schädel, C., Blöchl, A., Richter, A., and Hoch, G. (2010). Quantification and monosaccharide composition of hemicelluloses from different plant functional types. *Plant Physiol. Biochem.* 48, 1–8. doi: 10.1016/j.plaphy.2009.09.008

Schäfer, I. K., Bliedtner, M., Wolf, D., Kolb, T., Zech, J., Faust, D., et al. (2018). A $\delta^{13}C$ and $\delta^{2}H$ leaf wax record from the Late quaternary loess-paleosoil sequence El Paraíso, central spain. *Palaeogeogr. Palaeoclimatol. Palaeoecol.* 507, 52–59. doi: 10.1016/j.palaeo.2018.06.039

Schimmelmann, A., Sessions, A. L., and Mastalerz, M. (2006). Hydrogen isotopic (D/H) composition of organic matter during diagenesis and thermal maturation. *Annu. Rev. Earth Planet. Sci.* 34, 501–533. doi: 10.1146/annurev.earth.34.031405.125011

Schmidt, M. W. I., Torn, M. S., Abiven, S., Dittmar, T., Guggenberger, G., Janssens, I. A., et al. (2011). Persistence of soil organic matter as an ecosystem property. *Nature* 478, 49–56. doi: 10.1038/nature10386

Sessions, A. L. (2016). Factors controlling the deuterium contents of sedimentary hydrocarbons. *Organ. Geochem.* 96, 43–64. doi: 10.1016/j.orggeochem.2016.02.012

Sessions, A. L., Burgoyne, T. W., Schimmelmann, A., and Hayes, J. M. (1999). Fractionation of hydrogen isotopes in lipid biosynthesis. *Organ. Geochem.* 30, 1193–1200. doi: 10.1016/S0146-6380(99)00094-7

Strobel, P., Haberzettl, T., Bliedtner, M., Struck, J., Glaser, B., Zech, M., et al. (2020). The potential of $\delta^{2}H_{n\text{-alkanes}}$ and $\delta^{18}O_{sugar}$ for paleoclimate reconstruction – A regional calibration study for South Africa. *Sci. Total Environ.* 716:137045. doi: 10.1016/j.scitotenv.2020.137045

Struck, J., Bliedtner, M., Strobel, P., Schumacher, J., Bazarradnaa, E., and Zech, R. (2020). Leaf wax *n*-alkane patterns and compound-specific $\delta^{13}C$ of plants and topsoils from semi-arid and arid Mongolia. *Biogeosciences* 17, 567–580. doi: 10.5194/bg-17-567-2020

Thomas, E. K., Huang, Y., Clemens, S. C., Colman, S. M., Morrill, C., Wegener, P., et al. (2016). Changes in dominant moisture sources and the consequences for hydroclimate on the northeastern Tibetan Plateau during the past 32 kyr. *Quatern. Sci. Rev.* 131, 157–167. doi: 10.1016/j.quascirev.2015.11.003

Tipple, B. J., and Pagani, M. (2013). Environmental control on eastern broadleaf forest species' leaf wax distributions and D/H ratios. *Geochim. Cosmochim. Acta* 111, 64–77. doi: 10.1016/j.gca.2012.10.042

Trabucco, A., and Zomer, R. (2019). *Global Aridity Index and Potential Evapotranspiration (ET0) Climate Database version 2*.

Tuthorn, M., Zech, M., Ruppenthal, M., Oelmann, Y., Kahmen, A., Valle, H. F. D., et al. (2014). Oxygen isotope ratios ($^{18}O/^{16}O$) of hemicellulose-derived sugar biomarkers in plants, soils and sediments as paleoclimate proxy II: insight from a climate transect study. *Geochim. Cosmochim. Acta* 126, 624–634. doi: 10.1016/j.gca.2013.11.002

Tuthorn, M., Zech, R., Ruppenthal, M., Oelmann, Y., Kahmen, A., del Valle, H. F., et al. (2015). Coupling $\delta^{2}H$ and $\delta^{18}O$ biomarker results yields information on relative humidity and isotopic composition of precipitation – a climate transect validation study. *Biogeosciences* 12, 3913–3924. doi: 10.5194/bg-12-3913-2015

Vogts, A., Badewien, T., Rullkötter, J., and Schefuß, E. (2016). Near-constant apparent hydrogen isotope fractionation between leaf wax *n*-alkanes and precipitation in tropical regions: evidence from a marine sediment transect off SW Africa. *Organ. Geochem.* 96, 18–27. doi: 10.1016/j.orggeochem.2016.03.003

Wang, W., and Feng, Z. (2013). Holocene moisture evolution across the Mongolian Plateau and its surrounding areas: a synthesis of climatic records. *Earth Sci. Rev.* 122, 38–57. doi: 10.1016/j.earscirev.2013.03.005

Yamanaka, T., Tsujimura, M., Oyunbaatar, D., and Davaa, G. (2007). Isotopic variation of precipitation over eastern Mongolia and its implication for the atmospheric water cycle. *J. Hydrol.* 333, 21–34. doi: 10.1016/j.jhydrol.2006.07.022

Zech, M., and Glaser, B. (2009). Compound-specific $\delta^{18}O$ analyses of neutral sugars in soils using gas chromatography-pyrolysis-isotope ratio mass spectrometry: problems, possible solutions and a first application. *Rapid Commun. Mass Spectr.* 23, 3522–3532. doi: 10.1002/rcm.4278

Zech, M., Pedentchouk, N., Buggle, B., Leiber, K., Kalbitz, K., Markoviæ, S. B., et al. (2011). Effect of leaf litter degradation and seasonality on D/H isotope ratios of *n*-alkane biomarkers. *Geochim. Cosmochim. Acta* 75, 4917–4928. doi: 10.1016/j.gca.2011.06.006

Zech, M., Werner, R. A., Juchelka, D., Kalbitz, K., Buggle, B., and Glaser, B. (2012). Absence of oxygen isotope fractionation/exchange of (hemi-) cellulose derived sugars during litter decomposition. *Organ. Geochem.* 42, 1470–1475. doi: 10.1016/j.orggeochem.2011.06.006

Conflict of Interest: The authors declare that the research was conducted in the absence of any commercial or financial relationships that could be construed as a potential conflict of interest.